Zeitschrift für Physikalische Chemie, Bd. 208, S. 93–106 (1999)

Growth and Magnetism of Ultrathin Electrodeposited Co Films*

By W. Schindler, Th. Koop and J. Kirschner

Max-Planck-Institut für Mikrostrukturphysik, Weinberg 2, D-06120 Halle, Germany

(Received October 29, 1997; accepted December 1, 1997)

Electrodeposition / Ultrathin magnetic films / Co, Cu / Magneto-optical Kerr effect / X-ray diffraction

Ultrathin Co films have been electrodeposited onto Cu(001) single crystals from a deaerated aqueous electrolyte of 0.3 M Na_2SO_4 and 1 mM $CoSO_4$. The films show the intrinsic magnetic properties of Co, as measured *in situ*, if the cleanliness conditions in the electrochemical cell are equivalent to ultrahigh vacuum conditions. The combination of magneto-optical Kerr effect (MOKE) measurements and surface X-ray diffraction with an electrochemical cell allows us to monitor *in situ* the magnetic hysteresis of the films, their epitaxial properties, their growth and dissolution, as well as their stability near the Nernst potential of Co^{2+}/Co. Unlike with the scanning tunneling microscope, magnetic properties, as e.g. the coercivity, or structural properties of buried layers or the Co/Cu interface can be obtained, which complement the electrochemical measurements. Films thicker than 1.5 ML show their easy magnetization-axis in-plane and parallel [110]. The magnetic moment increases linearly with the film thickness. The measured magnetic anisotropies originate from the symmetry of the fcc crystal structure and demonstrate the epitaxial growth of electrodeposited Co on Cu(001).

1. Introduction

The growth of thin non-magnetic 3d-metal films on noble metal single crystal surfaces has been investigated in detail in the recent years. In particular the underpotential deposition of metals, as e.g. Cu, on noble metal surfaces like Ag(111) or Au(111) has been studied extensively [1]. However, electrodeposited magnetic 3d-metal films have been studied mainly in the thickness regime above 100 nm [2]. Ultrathin magnetic films in the monolayer

* Presented at the *5. Ulmer Elektrochemische Tage* on „Fundamental Aspects of Electrolyte Metal Deposition", June 23–24, 1997.

(ML) thickness range have been prepared so far preferably in ultrahigh vacuum by evaporation or sputtering techniques. One major reason for this fact is the strong influence of film impurities on the magnetic properties. Early experiments, more than 25 years ago, electrodepositing ultrathin Fe, Co and Ni films resulted in the finding of 'magnetically dead' atomic layers [3, 4], which spurred big efforts to investigate this fundamental 'novel effect' in more detail. However, by the time it became clear from films deposited under ultrahigh vacuum conditions that these 'novel effects' were caused by impurities in the electrodeposited films.

Since then, ultrathin magnetic films and multilayers have attracted more interest even from the point of view of possible applications as magnetic sensors in the automobile industry or biotechnology, or as storage media of much higher density than 10^8 bit/cm^2, which is state of the art today [5]. These applications require film thicknesses much below 1 μm or magnetic multilayers with single layer thicknesses in the nm range, which can be prepared by electrodeposition [6–8]. The electrodeposition with its benefits of large area deposition, low material consumption, suitability for mass production, fast processing, and low cost of equipment, seems to be much better suited to produce such films or structures than the deposition techniques requiring ultrahigh vacuum.

In this paper we will focus on the growth of Co on Cu(001) single crystals as an example for the overpotential deposition of ultrathin magnetic films onto a non noble single crystal working electrode (WE), and their properties as measured *in situ* in the electrochemical cell. We will show, that magnetic films in the monolayer range, showing the intrinsic magnetic properties as known from high quality evaporated films, can be electrodeposited on Cu(001) under ultrapure conditions. In particular the *in situ* measurements of the magnetic properties of the films using magneto-optical Kerr effect (MOKE), which has been combined with an electrochemical cell, is a powerful complement of the electrochemistry. This technique allows us to measure structural properties of films in the case of epitaxial growth. The structure of thin films is usually determined by electron diffraction at different electron energies (LEED, MEED, RHEED), X-ray diffraction or in real space by scanning tunneling microscopy (STM). Electron diffraction cannot be applied in an electrochemical cell, since electrons cannot penetrate liquids. Structure determination from STM images requires sub-Å resolution, which appears hard to achieve in the presence of an aqueous electrolyte at the surface of Fe, Co or Ni films. Surface X-ray diffraction, however, provides a FWHM resolution of approximately 0.001 Å, the highest resolution among the techniques mentioned, and is furthermore applicable *in situ* in the electrolyte. We will show the possibilities of the surface X-ray diffraction technique by studying *in situ* the epitaxial properties of our Co films.

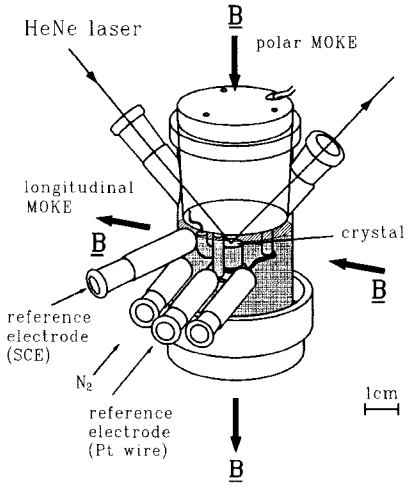

Fig. 1. Electrochemical quartz glass cell developed for *in situ* MOKE measurements. The cell fits between the pole pieces of an electromagnet which provides a magnetic field of 0.5 T at the position of the working electrode.

2. Experimental details

The electrochemical measurements have been performed in an electrochemical cell (Fig. 1), which provides cleanliness conditions during film deposition and *in situ* measurements equivalent to ultrahigh vacuum conditions of 5×10^{-10} mbar [9]. The details of the cell design, which is compatible with *in situ* MOKE measurements (see section 5), have been reported in Ref. [10]. The clean preparation conditions are of importance since the magnetic properties of ultrathin films react sensitively on impurities. Unclean preparation conditions would result in strange magnetic properties [3, 4], as mentioned above.

We achieve these conditions by using a quartz glass cell, by carefully cleaning all parts of the cell with H_2SO_4/H_2O_2 and sterilizing in ultrapure water before each experiment. We use suprapure grade reagents and remove carefully *in situ* dissolved oxygen from the aqueous electrolyte by bubbling with 5 N N_2 gas to prevent oxidation of the Co or Cu surfaces. A second reason for deaerating the electrolyte is to achieve a charge resolution equivalent of 0.02 ML from the cyclic voltammogram, which could not be achieved in the presence of oxygen [11]. We do not use additives to avoid, e.g., surfactant effects or other unknown influences on the growth of the films.

The Cu crystals were oriented and mechanically polished to better than 0.2° deviation from the Cu(001) plane which has been verified by X-ray diffraction. All areas of the Cu crystals except the oriented surface were

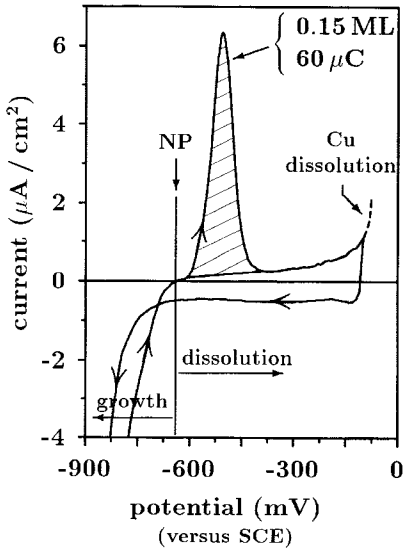

Fig. 2. Cyclic voltammogram of the Co deposition from deaerated 0.3 M Na_2SO_4/1 mM $CoSO_4$. The potentials are measured with respect to a saturated calomel electrode (SCE). The arrows indicate the cycling direction of the voltage sweep with 10 mV/s. The current between −100 mV and −600 mV is mainly caused by the charging of the electrochemical double layer during the voltage sweep. The anodic peak around −500 mV (dashed area) corresponds to a previously deposited charge of 60 μC or 0.15 ML thickness. MOKE is done *in situ* with the potential held at the Nernst potential ('NP').

isolated with a commercial lacquer to prevent contact of ill-defined parts of the crystal with the electrolyte. The surface of the Cu crystals was electrochemically polished in 65% H_3PO_4 at potentials of +1.8 V against a graphite electrode for several minutes. The crystals were then carefully rinsed with ultrapure water (Milli-Q plus) and transferred into the electrochemical cell under protection of a drop of ultrapure water. They were then immediately connected to the potentiostat at −200 mV versus a saturated calomel reference electrode (SCE) to provide cathodic protection of the Cu surface. The pH-value of the aqueous electrolyte was 4.5−5. All potentials in this paper are quoted with respect to SCE.

3. Cyclic voltammetry

The cyclic voltammogram of Co on Cu(001) from 0.3 M Na_2SO_4 and 1 mM $CoSO_4$ is shown in Fig. 2. The Nernst potential of 1 mM Co^{2+}/Co is −640 mV versus the saturated calomel electrode (SCE), as indicated in

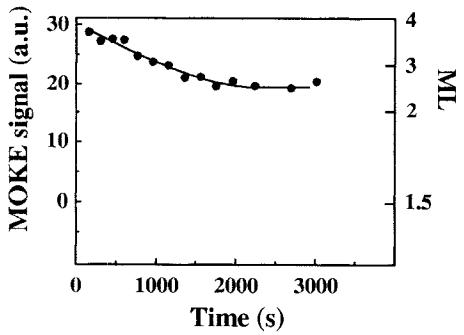

Fig. 3. Time dependence of the MOKE signal (left y axis) and the ML equivalent (right y axis) for a 3.9 ML Co film. Cell potential at −630 mV, slightly higher than the Nernst potential of Co^{2+}/Co, and hence resulting in a decrease of the Co coverage with time. The thickness variation at this cell potential is approximately 1.5 ML per hour. (**B**||[110], in-plane; T = 300 K).

Fig. 2 by 'NP'. We observe an overpotential deposition of Co on Cu(001) which is accompanied by a simultaneous H_2 evolution at potentials lower than −650 mV.

The cyclovoltammogram of the Co deposition shows a capacitive current of less than 0.6 μA/cm² in the double layer range between −100 mV and −650 mV (Fig. 2). There is neither oxidation nor oxide removal from the clean Cu(001) surface seen, which would be expected around −550 mV [12]. The clean and non-oxidized Cu surface has been checked in each experiment by multiple cycling of the potential between −400 mV and −10 mV. The anodic and cathodic charges due to the dissolution and subsequent redeposition of Cu were equal in all measurements. In the potential range of Fig. 2, we do neither observe electrosorption of oxygen species (for example $Cu\text{-}(OH)_{ads}$) at the Cu(001) surface [13] nor adsorption or phase transition phenomena, which is in agreement with previous studies of Cu(001) electrodes in a HCl electrolyte [14, 15].

The H_2 evolution during the Co deposition results in a non-balance of cathodic (integral of negative current during film deposition (Fig. 2)) and anodic charges (integral of positive current peak due to the film dissolution (Fig. 2)) in the cyclic voltammogram. Whereas the cathodic charge represents the sum of charges due to hydrogen reduction and film deposition, the anodic charge (dashed peak area in Fig. 2) results exclusively from the film dissolution. Therefore, the deposited coverage can be determined with an accuracy of 0.02 ML from the anodic charge, the geometrical area of the WE, and the bulk fcc-Co lattice constant of 0.354 nm. Nevertheless, the cathodic charge can be calibrated with the corresponding anodic charge in several deposition/dissolution cycles.

Thus, by the adjustment of the substrate potential we can simply control growth or dissolution of the films. In particular, we can hold the films in a stable condition with respect to their thickness, if we adjust the potential of the substrate at the Nernst potential of Co^{2+}/Co, as indicated in Fig. 2 by 'NP'.

The stability of films under these conditions for up to one hour has been proven by using *in situ* MOKE to monitor independently the saturation magnetization of the film, which has been found to be proportional to its thickness [16], if the film thickness is smaller than the penetration depth of the light. This is fulfilled for film thicknesses below 50 ML and visible light. The stability of films near the Nernst potential is an essential requirement for the *in situ* application of those analytical techniques, which require long measurement times, as e.g. X-ray diffraction (see section 5).

The time dependence of the MOKE signal of a 3.9 ML thick Co film held at a potential of −630 mV, approximately 10 mV above the Nernst potential of Co^{2+}/Co, is shown in Fig. 3. The film thickness decreases by 1.5 ML within 50 minutes. The dissolved anodic charge after the long time MOKE measurement of Fig. 3 was equivalent to a film thickness of 2.4 ML in good agreement with the MOKE measurement.

Increase or decrease of the MOKE signal, corresponding to increase or decrease of the Co coverage, can be easily controlled by adjusting the potential slightly lower or higher in the range around the Nernst potential. This opens interesting prospects for the preparation of ultrathin films with tailored magnetic properties in view of potential applications as magneto-resistive sensors, in the storage technology, or in complex multilayered systems.

4. Magneto-optical KERR measurements

The MOKE measurements are performed *in situ* using the same electrochemical cell (Fig. 1) as taken for the cyclic voltammetry. The cell fits between the pole pieces of an electromagnet, which provides a magnetic field of up to 0.5 T at the WE position. The magnet is rotatable to adjust the magnetic field in different crystallographic orientations of the films to be able to determine different in-plane and out-of-plane magnetization components of the films. The magnetization is measured using a 1 mW HeNe laser, providing linearly polarized light, and a lock-in modulation technique [16] to measure the rotation of the polarization vector of the light by the film magnetization. The magnetic moment of the film volume probed by the light spot is proportional to the MOKE signal. The area of the unfocused laser spot on the Cu(001) surface is approximately 1 mm^2, which allows us to investigate large surface areas. The magnetization measurements can be done at room temperature without removing the Co films from the liquid.

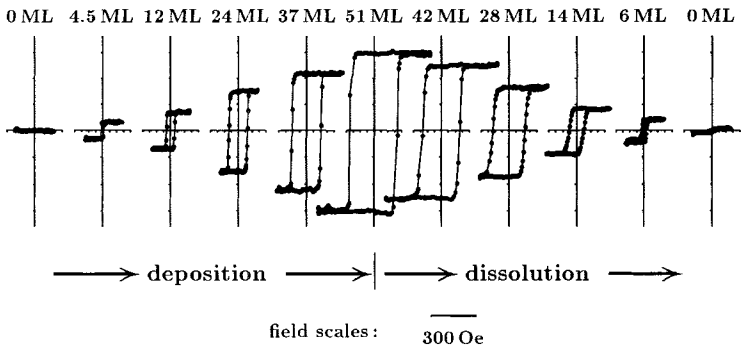

Fig. 4. Magnetic hysteresis loops (at room temperature) during deposition and subsequent dissolution of a single Co film. The magnetic field was aligned in-plane and along the easy [110] magnetization direction.

The latter is of importance since the magnetic properties of films in the ML range may be drastically changed by oxidation in air in the case of *ex situ* magnetization measurements. *In situ* deposited capping layers to protect the films may result in strikingly different magnetic properties [17] compared to films without capping layers. The in-plane magnetization anisotropy has been measured by rotating the Cu crystal about the [001] axis (film normal) with the applied magnetic field and optical MOKE setup fixed.

4.1 Reversibility

Growth and dissolution of a single film has been observed *in situ* by measuring its magnetic properties *in situ*, see Fig. 4. In general, MOKE can be performed simultaneously with the growth or dissolution of films; however this results in non-closed hysteresis loops due to the difference of the film thicknesses at the beginning and at the end of the MOKE measurement. Therefore, in order to achieve a constant film thickness during each MOKE measurement in Fig. 4, we interrupted growth and dissolution for approximately 20–30 s by switching the Cu potential to the Nernst potential of Co^{2+}/Co where the film thickness remains constant, as indicated in Fig. 2 by 'NP'. The square magnetic hysteresis (remanence = saturation magnetization) during the deposition suggests a uniform Co film thickness across the measured surface area of approximately 1 mm^2, whereas the increasing rounding of the hysteresis loops during the dissolution of the film might be caused by a slightly inhomogeneous dissolution across the substrate area, which would result in a non-uniform thickness distribution and hence the observed rounding of the square hysteresis.

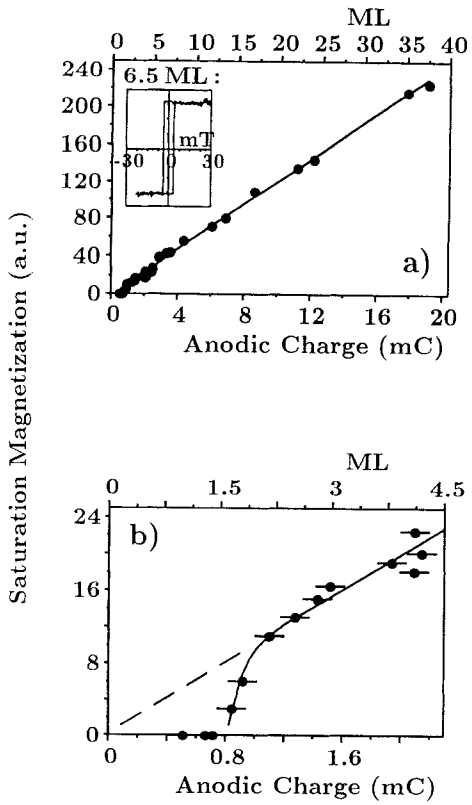

Fig. 5. Linear dependence of the magnetic moment on the film thickness. Since the MOKE signal depends linearly on the deposited charge at thicknesses above 2 ML, it can be taken as a complementary thickness measure besides the electrochemical charge measurement. (a) thickness range 0–50 ML; (b) expanded thickness range 0–4.5 ML.

In particular, the Co films can be completely removed from the Cu(001) surface if the substrate potential is adjusted around approximately −300 mV according to the cyclic voltammogram of Co (Fig. 2). Correspondingly, the magnetic hysteresis vanishes, as is shown in Fig. 4.

4.2 Saturation magnetization

At room temperature we observe a magnetization in films thicker than 1.5 ML (Fig. 5). The linear dependence of the saturation magnetization on the film thickness is plotted in detail in Fig. 5a. This linearity proves that MOKE can be taken as independent measure of the film thickness complementary to the charge integral of the dissolution peak in Fig. 2. The

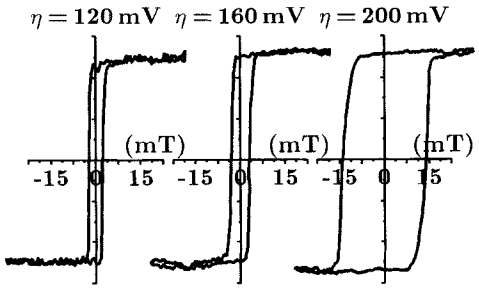

Fig. 6. Enhancement of the coercivity caused by deposition at high supersaturation η. Vertical scales are the same for all graphs (a.u.). The film thickness is 6 ML (**B**||[110], in-plane; T = 300 K).

vanishing magnetic hysteresis below 2 ML (Fig. 5b) is caused by the decrease of the Curie temperature with decreasing film thickness, since all measurements have been performed at room temperature. This thickness dependence of the Curie temperature is known from evaporated ultrathin magnetic films [18]. The onset of the magnetization around 1.5 ML and the square magnetic hystereses are compatible with a layer-by-layer growth mode in the initial stages of the deposition.

4.3 Coercivity

Whereas the saturation magnetization increases linearly with film thickness, the increase of the coercivity with film thickness is not linear because of the complex mechanisms of the magnetization reversal in ultrathin films, which are closely related to the microstructural properties of the films. This can be clearly demonstrated by preparing films at different supersaturation and hence at different deposition current densities. The increase of the coercivity due to the very rapid deposition at high supersaturation is shown in Fig. 6 for films of same thickness (6 ML), deposited at different overpotentials η. The coercivity of film deposited at high supersaturation (η = 200 mV; right curve in Fig. 6) is approximately 7 times larger than the coercivity of the film deposited at a low supersaturation (η = 120 mV; left curve in Fig. 6). These strikingly different magnetic properties are one example of the importance of complementary measurements of the physical film properties, particularly in our case of magnetic films.

4.4 Magneto-crystalline anisotropy

The easy magnetization direction in our Co films is in-plane as has been shown earlier [9]. The epitaxy of the films on Cu(001) can be observed by X-ray diffraction, as will be shown below, but can even be inferred from

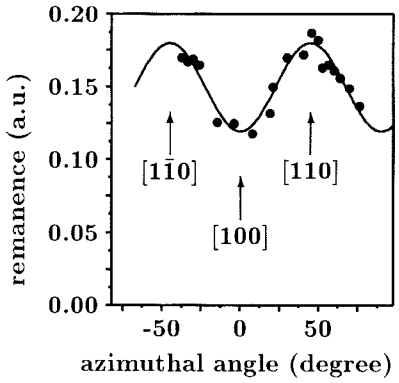

Fig. 7. In-plane anisotropy of the remanent magnetization of 13 ML Co on Cu(001) (T = 300 K). The azimuthal angle is measured with respect to the hard [100] direction.

anisotropy measurements done *in situ* by rotating the crystal about its normal with the magnetic field kept in-plane. As shown in Fig. 7, the remanence, i.e. the magnetization at zero field, shows a fourfold symmetry. This fourfold symmetry has also been found in films grown by molecular beam epitaxy (MBE) in ultrahigh vacuum [19] which were structurally characterized by electron diffraction. We find two easy in-plane axes in the [110] and [1$\underline{1}$0] directions, whereas the hard axes are in the [100] and [010] directions, respectively. The lower remanence corresponds to the hard magnetization axis, in our case the [100] and [010] directions, due to the fcc Co film structure. These same observations have been made on MBE films. From this close similarity we conclude that our electrochemically deposited films maintain the same epitaxial relationship with the substrate and have the same crystalline structure. The epitaxial growth as shown in Fig. 7 has been checked on an area of the order of 1 mm^2, which is the size of our laser beam on the sample surface. Such a large area cannot be structurally investigated by means of atomically resolved electrochemical STM. Thus, MOKE can be advantageously taken to determine structural properties on large scales compared to STM.

5. X-ray diffraction

A second method to investigate epitaxial properties of films is *in situ* surface X-ray diffraction in a special electrochemical thin electrolyte layer cell (Fig. 8). High resolution X-ray diffraction in an electrochemical cell requires a thin electrolyte layer geometry with a highly X-ray transparent Mylar window in front of the WE surface to provide low X-ray absorption. Our cell design (Fig. 8) [11] allows additionally the *in situ* deaeration of

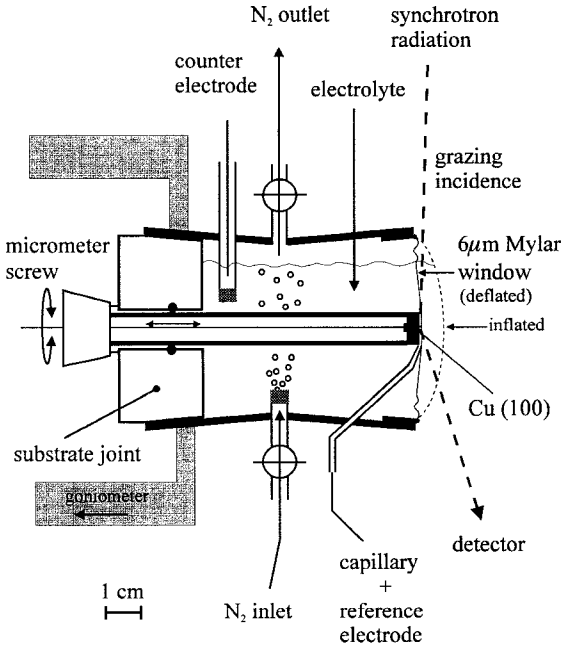

Fig. 8. Electrochemical thin electrolyte layer cell developed for the *in situ* surface X-ray diffraction measurements. The cell can be rotated about its horizontal axis by 360°. The gas bubbles do not affect the different electrodes.

the aqueous electrolyte and a transfer of the Cu crystal from and into the cell protected from air, to achieve the same cleanliness conditions as mentioned above in section 1. The bubbling of N_2 was stopped during the X-ray diffraction measurements. The potential was adjusted to −250 mV during the alignment of the crystal on the diffractometer at the BW2 beamline at HASYLAB (DESY, Hamburg). We used a photon energy of 8.5 keV, approximately 0.5 keV below the K-edge of Cu. The X-ray angle of incidence was chosen to 0.3°, close to the total reflection angle of Cu, in order to achieve a high surface sensitivity. Measurements have been done near the [2,−2,0] in-plane reflection of fcc Cu(001), to investigate the in-plane lattice constant of fcc Co at different coverages.

The sequence of diffraction measurements in Fig. 9 on clean Cu(001), 8.5 ML Co/Cu(001), and 12.5 ML Co/Cu(001) shows the evolution of the lineshape of the [2,−2,0] in-plane reflection with increasing Co coverage. At 8.5 ML (Fig. 9b) we observe a broadening of the Cu peak caused by pseudomorphically grown Co, which has exactly adopted the in-plane lattice constant of fcc Cu, as indicated by the dotted fit curve in Fig. 9b. The peak shoulder in Fig. 9b at larger reciprocal lattice vectors is caused by Co which

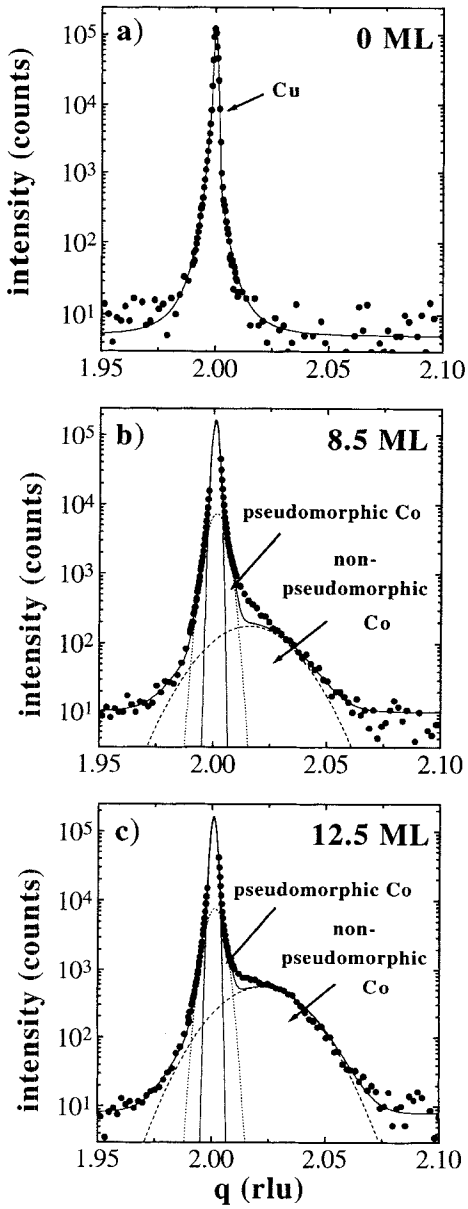

Fig. 9. In-plane [2,−2.0] X-ray diffraction peaks (X-ray intensity versus relative wave vector q in [2,−2.0] direction) for clean Cu(001) (a), 8.5 ML Co/Cu(001) (b), and 12.5 ML Co/Cu(001) (c), showing the pseudomorphic growth in the initial growth stages, and the subsequent in-plane lattice constant relaxation with increasing Co coverage. Dotted lines: pseudomorphic Co; dashed line: non-pseudomorphic Co; solid lines: contribution of the Cu substrate and sum of all curves.

grows already with a relaxed in-plane lattice constant, as modelled by the dashed fit curve in Fig. 9b. This second peak becomes clearer at higher coverages (Fig. 9c) and shifts to a larger reciprocal lattice vector (corresponding to a smaller lattice constant), as indicated by the dashed fit curve in Fig. 9c. However, the pseudomorphically grown Co layers remain visible in the diffraction peak of the 12.5 ML film, as indicated by the dotted line in Fig. 9c. Thus, it is possible to observe directly the structure of buried layers or interfaces, which is hardly possible using other techniques. The detailed crystallographic investigation of Co/Cu(001) will be published in [20].

6. Conclusion

The electrodeposition of ultrathin magnetic Co films in the monolayer range requires cleanliness conditions equivalent to ultrahigh-vacuum conditions. We have shown in this paper, that the electrochemical characterization techniques can be significantly complemented, if combined with *in situ* measurement techniques like MOKE and X-ray diffraction. This is particularly interesting in the case of studiing ultrathin films in the ML range. Structural information can be deduced indirectly, e.g., from magnetic anisotropies or directly from X-ray diffraction, which provides not only top layer sensitivity, but also information about the structure of buried layers or interfaces. The saturation magnetization is found to be an independent measure of the film thickness due to its linear dependence on the deposited charge. The magnetic coercivity has been shown to be significantly altered by the deposition parameters. From the complementary *in situ* investigation of the magnetic in-plane anisotropy we can deduce, in addition to electrochemical growth studies, and in agreement with X-ray diffraction, that our Co films grow epitaxially in fcc structure on large scales of several mm^2 on Cu(001).

Acknowledgements

We are indebted to H. Menge for the preparation of the Cu crystals and the steady maintenance of our water purification system. The X-ray diffraction experiments have been a collaboration with J. Zegenhagen, G. Scherb, and A. Kazimirov from MPI für Festkörperforschung, Stuttgart, and with R. Feidenhans'l and Th. Schultz from Risø National Laboratory, Denmark. We would like to thank the staff of HASYLAB and DESY for their assistance in the X-ray diffraction experiments.

References

1. E. Budevski, G. Staikov, and W. J. Lorenz, *Electrochemical Phase Formation and Growth* (VCH, Weinheim 1996); M. H. Hölzle, V. Zwing, and D. M. Kolb, Electrochim. Acta **40** (1995) 1237.

2. S. Yoshimura, S. Yoshihara, T. Shirakashi, and E. Sato, Electrochim. Acta **39** (1994) 589; D. Y. Li and J. A. Szpunar, J. Mat. Science **28** (1993) 5554; G. Pimenta, V. Schröder, and W. Kautek, Ber. Bunsenges. Phys. Chem. **95** (1991) 1470; Y. Jyoko, S. Kashiwabara, and Y. Hayashi, Materials Transactions, JIM **33** (1992) 211; C. Wisniewski, I. Denicolo, and I. A. Hümmelgen, J. Electrochem. Soc. **142** (1995) 3889.
3. L. N. Liebermann, D. R. Fredkin and H. B. Shore, Phys. Rev. Lett. **22** (1969) 539.
4. L. N. Liebermann, J. Clinton, D. M. Edwards, and J. Mathon, Phys. Rev. Lett. **25** (1970) 232.
5. J. L. Simonds, Physics Today **48** (April 1995) 26.
6. M. Alper, K. Attenborough, R. Hart, S. J. Lane, D. S. Lashmore, C. Younes, and W. Schwarzacher, Appl. Phys. Lett. **63** (1993) 2144.
7. S. K. J. Lenczowski, C. Schönenberger, M. A. M. Gijs and W. J. M. de Jonge, J. Magn. Mag. Mat. **148** (1995) 455.
8. K. D. Bird and M. Schlesinger, J. Electrochem. Soc. **142** (1995) L65.
9. W. Schindler and J. Kirschner, Phys. Rev. B **55** (1997) R1989.
10. W. Schindler and J. Kirschner, Rev. Sci. Instrum. **67** (1996) 3578.
11. Th. Koop, W. Schindler, A. Kazimirov, G. Scherb, J. Zegenhagen, Th. Schulz, R. Feidenhans'l, and J. Kirschner, Rev. Sci. Instrum. **69** (1998) 1840.
12. U. Bertocci and D. D. Wagman, in *Standard Potentials in Aqueous Solution*, edited by A. J. Bard, R. Parsons and J. Jordan (Marcel Dekker, New York 1985) p. 287.
13. S. Härtinger and K. Doblhofer, J. Electroanal. Chem. **380** (1995) 185.
14. C. B. Ehlers, I. Villegas and J. L. Stickney, J. Electroanal. Chem. **284** (1990) 403.
15. M. R. Vogt, F. A. Möller, C. M. Schilz, O. M. Magnussen and R. J. Behm, Surf. Sci. **367** (1996) L33.
16. S. D. Bader, J. Magn. Mag. Mat. **100** (1991) 440.
17. C. Chappert and P. Bruno, J. Appl. Phys. **64** (1988) 5736; J. Ferre, G. Penissard, C. Marliere, D. Renard, P. Beauvillain, J. P. Renard, Appl. Phys. Lett. **56** (1990) 1588; M. Speckmann, H. P. Oepen, and H. Ibach, Phys. Rev. Lett. **75** (1995) 2035.
18. C. M. Schneider, A. K. Schmid, H. P. Oepen, and J. Kirschner, in *Magnetism and Structure in Systems of Reduced Dimensions*, edited by R. G. F. Farrow, B. Dieny, M. Donath, A. Fert, B. Hermsmeier (Plenum Press, New York 1993) p. 453.
19. M. Kowalewski, C. M. Schneider, and B. Heinrich, Phys. Rev. B **47** (1993) 8748.
20. W. Schindler, Th. Koop, A. Kazimirov, G. Scherb, J. Zegenhagen, Th. Schulz, R. Feidenhans'l, and J. Kirschner, to be published (1998).